Biometals (2012) 25:553–561
DOI 10.1007/s10534-012-9534-x

Delineation of the molecular mechanism for disulfide stress-induced aluminium toxicity

Ming J. Wu · Patricia A. Murphy · Patrick J. O'Doherty · Stephen Mieruszynski · Mark Jones · Cindy Kersaitis · Peter J. Rogers · Trevor D. Bailey · Vincent J. Higgins

Received: 18 December 2011 / Accepted: 22 February 2012 / Published online: 9 March 2012

Abstract Following our previous finding that the sulfhydryl-oxidising chemical diamide induced a marked elevation of cellular Al^{3+} (Wu et al., Int J Mol Sci, 12:8119–8132, 2011), a further investigation into the underlying molecular mechanism was carried out, using the eukaryotic model organism *Saccharomyces cerevisiae*. The effects of non-toxic dose of diamide (0.8 mM) and a mild dose of aluminium sulphate (Al^{3+}) (0.4 mM) were determined prior to the screening of gene deletion mutants. A total of 81 deletion mutants were selected for this study according to the available screening data against Al^{3+} only (Kakimoto et al., BioMetals, 18: 467–474, 2005) and diamide only (Thorpe et al., Proc Natl Acad Sci USA, 101: 6564–6569, 2004). On the basis of our screening data and the cluster analysis, a cluster containing the gene deletions (*rpe1Δ*, *sec72Δ*, *pdr5Δ* and *ric1Δ*) was found to be specifically sensitive to the mixture of diamide and Al^{3+}. However *gnp1Δ*, *mch5Δ* and *ccc1Δ* mutants were resistant. Dithiothreitol (DTT) and ascorbate markedly reversed the diamide-induced Al^{3+} toxicity. Inductively-coupled plasma optical emission spectrometry demonstrated that DTT reduced the intracellular Al^{3+} content in diamide/Al^{3+}-treated yeast cells six-fold compared to the non-DTT controls. These data together revealed that the pleiotropic drug resistance transporter (Pdr5p) and vacuolar/vesicular transport-related proteins (Ric1p and Sec72p) are the targets of diamide. A dysfunctional membrane-bound Pdr5p terminates the detoxification pathway for Al^{3+} at the final step, leading to intracellular Al^{3+} accumulation and hence toxicity. As Al^{3+} toxicity has been a problem in agriculture and human health, this study has provided a significant step forward in understanding Al^{3+} toxicity.

Keywords Disulfide stress · Diamide · Aluminium · Toxicity · Yeast

Electronic supplementary material The online version of this article (doi:10.1007/s10534-012-9534-x) contains supplementary material, which is available to authorized users.

M. J. Wu (✉) · P. A. Murphy · P. J. O'Doherty · S. Mieruszynski · M. Jones · C. Kersaitis · T. D. Bailey
School of Science and Health, University of Western Sydney, Locked Bag 1797, Penrith, NSW 2751, Australia
e-mail: m.wu@uws.edu.au

P. J. Rogers
Carlton and United Breweries, Fosters Group, 4-6 Southampton Crescent, Abbotsford, Melbourne 3067, Australia

Present Address:
P. J. Rogers
School of Science, Griffith University, Nathan, South Brisbane, QLD 4111, Australia

V. J. Higgins (✉)
Ramaciotti Centre for Gene Function Analysis, School of Biotechnology and Biomolecular Sciences, University of New South Wales, Sydney, NSW 2052, Australia
e-mail: v.higgins@unsw.edu.au

Introduction

Cysteine is arguably the most important residue for the structure and function of many cellular proteins (Nagahara 2011). Two cysteines may be oxidized to form an intra- or inter-protein disulfide. Exposure to oxidants may lead to the formation of exotic disulfide bonds within or between proteins of living organisms, resulting in a specific stress condition termed disulfide stress (Leichert et al. 2003). Diamide [diazene-dicarboxylic acid *bis*(*N*,*N*-dimethylamide)], a diazene derivative, is a membrane permeable and widely-used thiol-specific oxidant in oxidative research (Kosower and Kosower, 1995). Its reaction mechanism involves two steps. Firstly, the free thiol group in a protein is oxidised by diamide to form sulfenylhydrazine, and then this reacts with another free thiol group to form a disulfide bridge and a hydrazine derivative. En route to the cytoplasma, diamide crosses the plasma membrane and attacks membrane-bound proteins such as human erythrocyte spectrin (Becker et al. 1986). Once inside the cell, it is antagonized rapidly and specifically by the defensive antioxidant molecules such as glutathione. But any residual diamide can then target and oxidize proteins encountered along the way. Overall, a myriad of responses may occur in experimentally treated or naturally affected cells from gene expression to changes in the ionomic dynamics (Gasch et al. 2000; Thorpe et al. 2004; Wu et al. 2011).

Out of our ionomic profiling data (Wu et al. 2011), a specific association between diamide-induced disulfide stress and aluminium ion (Al^{3+}) accumulation was uncovered. At an arresting but non-lethal concentration to cell growth, diamide induced an elevated level of the intracellular Al^{3+}. This unprecedented linkage between the two toxicants may be relevant to some pathological conditions in humans. For instance in the case of Alzheimer's disease (AD), Al^{3+} has long been associated with the pathogenesis of AD (Yumoto et al. 2001; Exley 2006; Walton 2006), albeit controversially. This relationship has been one of the reasons we have pursued the genes involved in the diamide-induced Al^{3+} accumulation and studied the underlying molecular mechanisms responsible.

Currently, one set of data, obtained by deletion mutant phenotypic screening (Thorpe et al. 2004), is available to interpret genome-wide responses of *Saccharomyces cerevisiae* to diamide. Forty-eight gene deletion mutants were identified to be sensitive to diamide treatment, and these mutants are immediately relevant to this study in regard to whether a mild concentration of diamide could enhance their Al^{3+} sensitivity. A genome-wide screening of Al^{3+} tolerance in yeast has also been described (Kakimoto et al. 2005), in which 37 Al^{3+} tolerance genes were unraveled. So far, neither deletion mutant screening nor transcriptomic profiling has been carried out with combined treatments of diamide and Al^{3+}. However, the gene lists identified in these two datasets offer valuable clues for our study. Instead of going through the laborious and expensive screening of thousands of deletion yeast mutants, we selected 81 target gene deletions, including the 48 diamide sensitive and majority of the Al^{3+} sensitive mutants (Supplementary information 1), for screening under mild concentrations of diamide and Al^{3+}. The specific genes associated with the diamide-induced Al^{3+} uptake were then identified and the reversibility of the diamide-induced process was also demonstrated with the reducing agent dithiothreitol (DTT) and antioxidant ascorbate.

Materials and methods

Yeast strains and culture media

The *S. cerevisiae* strain BY4743 (*MATa/α; his3Δ1/his3Δ1; leu2Δ0/leu2Δ0; met15Δ0/MET15; lys2Δ0/LYS2; ura3Δ0/ura3Δ0*) and the deletion mutants used in this study were obtained from EUROSCARF (Frankfurt, Germany) (Brachmann et al. 1998).

BY4743 was streaked from a frozen glycerol stock to the YEPD agar plate containing 1 % yeast extract, 2 % peptone, 2 % D-glucose and 2 % agar, and grown at 30 °C for 48 h. Yeast culture was initiated by inoculation of a single colony from the agar plate into the minimal medium containing 2 % D-glucose, 0.17 % yeast nitrogen base with neither ammonium sulphate nor amino acids, 0.5 % ammonium sulphate, and supplemented with 10 mg L^{-1} adenine, 50 mg L^{-1} L-arginine, 80 mg L^{-1} L-aspartic acid, 20 mg L^{-1} L-histidine HCl, 50 mg L^{-1} L-isoleucine, 100 mg L^{-1} L-leucine, 50 mg L^{-1} L-lysine HCl, 20 mg L^{-1} L-methionine, 50 mg L^{-1} L-phenylalanine, 100 mg L^{-1} L-threonine, 50 mg L^{-1} L-tryptophan, 50 mg L^{-1} L-tyrosine, 140 mg L^{-1} L-valine and 20 mg L^{-1} uracil. The pH of the media was adjusted to 3.4 with 0.1 M

HCl. The culture was shaken at 150 rpm at 30 °C. Yeast growth was monitored by measuring the optical density at 600 nm (OD_{600}).

Determination of the concentrations of diamide and Al^{3+} for screening deletion mutants

The concentration of diamide and Al^{3+}, either in combination or individually, was titrated for diamide (0–5 mM) and Al^{3+} (0–3.2 mM) in 96-well plate configurations. The plates were incubated at 30 °C incubator with shaking at 750 rpm. Yeast growth was monitored by OD_{600} measurement every 2 h for 24 h using a microplate reader (Multiskan EX, Thermo Electron, USA).

Screening deletion mutants under dual stressors of diamide and Al^{3+}

According to the findings of the previous experiment, the combined treatment of 0.8 mM diamide with 0.4 mM Al^{3+} was carried out with the 81 selected yeast deletion mutants. Three controls were performed in parallel, including 0.8 mM diamide only, 0.8 mM Al^{3+} only, and the medium with neither diamide nor Al^{3+}. The stock 96-well plates for deletion *S. cerevisiae* mutants as well as BY4743 were first prepared by culturing each genotype in two replicate wells. These genotypes were then transferred into each of the three treatment and the control plates by the means of a 96-pin replicator. The starting yeast OD_{600} was then read using a microplate reader (Multiskan EX, Thermo Electron, USA). The yeast growth for each mutant was again measured at the end of 24 h incubation. The growth phenotype of each mutant and the wild BY4743 was measured by the fold change of the final OD_{600} over the initial reading. The yeast growth was further confirmed by transferring the suspension cultures from the 96-well plates to YEPD agar plates using a 96-pin replicator. The yeast spots were observed and photographed after 24 h incubation at 30 °C. The control of 0.8 mM diamide only was carried out because the major aim of this study was to investigate the effect of a mild dose of disulfide stress-inducing diamide on Al^{3+} toxicity. The underlying reason for using the control of 0.8 mM Al^{3+} rather than 0.4 mM Al^{3+} was that at this concentration yeast cells showed a degree of sensitivity whilst the growth was almost normal at 0.4 mM Al^{3+}.

Confocal fluorescence microscopic observation of deletion mutants under dual stressors of diamide and Al^{3+}

Yeast cells at OD_{600} of 1.0 were treated with 0.8 mM diamide plus 0.4 mM Al^{3+} for 1 h. The cells were then washed three times with 2 mM EDTA, three times with H_2O, and once with 0.1 M acetate buffer (pH 5.2). Cells were stained with 10 μM lumogallion [3-(2,4 dihydroxyphenylazo)-2-hydroxy-5-chlorobenzene sulfonic acid] or morin in 0.1 M acetate buffer for 1 h at 50 °C. The cells were washed three times with the acetate buffer prior to the confocal microscope examination. Still confocal fluorescence images were acquired using an inverted Leica True Confocal Scanner-Spectro-Photometer 5 (TCS-SP) fitted with a 63X (1.4NA) water immersion objective. An argon ion laser set to 20 % was used to view the lumogallion samples with the 488 nm pathway open at 5 % and emission was detected between 500 and 540 nm. For samples stained with morin a diode 405 nm laser set to 40 % was used and the spectra between 490 and 530 nm was used for detection.

Effect of DTT and ascorbate on diamide-induced Al^{3+} toxicity

To demonstrate whether DTT or ascorbic acid was able to reverse or reduce the effect of disulfide stress on Al^{3+} toxicity in *S. cerevisiae*, three sets of the yeast mutants were cultured in a microtitre plate in medium containing 0.8 mM diamide and 0.4 mM Al^{3+}. Either 0.4 mM DTT, 3.2 mM ascorbate or straight medium was added to each set of culture. The concentrations of 0.4 mM DTT and 3.2 mM ascorbate were pre-determined for their non-toxicity to normal yeast growth. After 24 h incubation, 5 μL of each well of the cultures were transferred onto YPD agar plates using 96-well multipin replicator. The cells were allowed to grow at 30 °C for 48 h prior to analysis.

Effect of DTT on diamide-induced Al^{3+} accumulation

Yeast cells were treated with 0.8 mM diamide only, 0.8 mM diamide and 0.4 mM Al^{3+}, 0.8 mM diamide and 0.4 mM Al^{3+} and 0.8 mM DTT. The yeast growth for each treatment was monitored by reading at OD_{600}. Samples (2 × 25 mL) were taken at 0, 5, 10, 15 and

20 h. ICP-OES analysis was carried out after the samples were processed as described below.

Inductively-coupled plasma optical emission spectrometry (ICP-OES) analysis

The yeast culture samples were centrifuged 4,000 × *g* for 10 min at 15 °C. Medium supernatant was aspirated using a vacuum. Yeast pellets were then washed twice with 30 mL of 2 μM EDTA, and twice with 30 mL of deionized water. On completion, yeast pellets were re-suspended in 1 mL of MilliQ water and transferred to pre-weighed Eppendorf tubes. The Eppendorf tubes were centrifuged at 10,000 × *g* for 5 min. Supernatants were discarded and the biomass of each sample was measured gravimetrically after drying the pellets in a 70 °C oven for 5 h. The average biomass of each yeast sample was calculated against the two replicates.

Yeast samples were digested prior to analysis by ICP-OES (Varian 720-ES series). Each sample was digested in 1 mL 65 % nitric acid (Suprapur Merck) for 24 h at 25 °C. The samples were vortexed and centrifuged for 10 min at 13,000 rpm. Each sample (100 μL) was diluted 100-fold to a total volume of 10 mL with MilliQ water. The Varian 720-ES consisted of an axial torch configuration and sample introduction system equipped with a Seaspray nebuliser and Twister cyclonic baffled spray chamber. The sample introduction system was fitted with a Y-piece which incorporated on-line dilution of samples and standards with an Yttrium internal standard solution. Data analysis was completed with ICP Expert II software. ICP standard element solutions for Al^{3+} at 0, 0.05, 0.2, 0.5, 1.0 ppm were prepared via appropriate dilutions of standard solutions in ultrapure water and nitric acid at the final concentration of 6.5 %(v/v).

Bioinformatic analysis of the deletion mutant data

The fold changes for each mutant in the four treatments were calculated as the ratio of OD_{600} at 24 h over OD_{600} at the start. This data file was then analysed by using MeV version 4.5 hierarchical clustering program (Saeed et al. 2006). Gene functionality in each cluster was identified using the Functional Specification Resource, FunSpec (http://www.funspec.med.utoronto.ca) or *Saccharomyces* Genome Database (http://www.sgd.org). These programs use a hypergeometric distribution to quantitatively assess functionally enriched gene ontology categories after input of a cluster of genes with a cut-off *p* value of 0.01.

Results and discussion

The appropriate concentrations of diamide and Al^{3+} were firstly determined for the combined screening. As shown in Fig. 1, yeast cells in 0.8 mM diamide alone exhibited initial mild growth toxicity but recovered completely after 16 h and even increased approximately 5 % at 24 h. Cells adapted to 0.4 mM Al^{3+} after 16 h, showing 4 % less growth at the end of incubation compared to the non- Al^{3+} control, while 0.8 mM Al^{3+} resulted in about 13 % growth inhibition, and 1.6 mM Al^{3+} 67 % inhibition. Thus, 0.4 mM Al^{3+} was a critical point; concentrations higher than this imparting pronounced toxicity to yeast cells and rising thereafter at an exponential rate. Under combined treatment of 0.8 mM diamide with 0.4 mM Al^{3+}, there was a 52 % reduction of growth. Thus, 0.8 mM diamide with 0.4 mM Al^{3+} is basically an IC_{50} (half maximal inhibitory concentration) commonly used in bioassays (Widestrand et al. 2003). Additionally, 0.8 mM diamide with 0.2 mM Al^{3+}, that is, dropping the Al^{3+} level by half, resulted in 19 % inhibition. Based on these results, 0.8 mM diamide and 0.4 mM Al^{3+} was considered to be an appropriate combination for picking up synergistic effects during mutant screening, linking Al^{3+} accumulation to specific gene(s) functionality.

In fact, what was observed was that the toxicity of Al^{3+} to yeast cells was markedly elevated by the simultaneous addition of a non-toxic dose of diamide. This almost certainly was considered to be due to the increased Al^{3+} uptake. This result indeed points to a marked synergistic effect of diamide and Al^{3+} on toxicity to yeast growth. To elucidate the underlining molecular mechanism, gene deletion mutants ($n = 81$) were screened in four conditions including diamide alone (0.8 mM), Al^{3+} alone (0.8 mM), diamide (0.8 mM) plus Al^{3+} (0.4 mM), and the control with neither of them.

The phenotypic growth data of the mutants measured by the fold change of the final OD_{600} over the initial reading are within the range of 1.0–10.0. A fold change of 1.0 means there was no growth at all for the mutant. The data analysis using hierarchical clustering

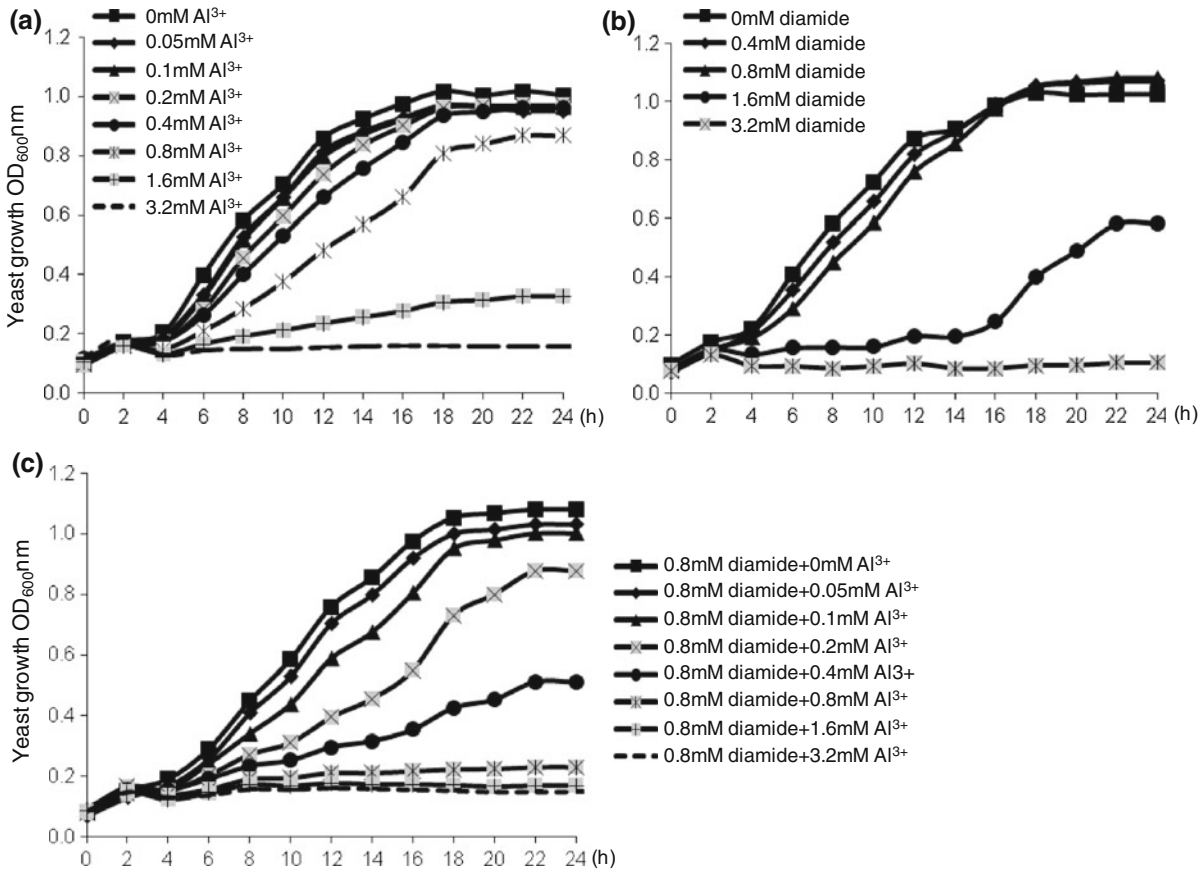

Fig. 1 Yeast growth curves for Al^{3+}, diamide and in combination. The effects of Al^{3+} and diamide on yeast growth. **a** Cell growth curves under a series of $Al_2(SO_4)_3$ concentrations (0, 0.05, 0.1, 0.2, 0.4, 0.8, 1.6 and 3.2 mM). **b** Cell growth under diamide treatment of 0, 0.4, 0.8, 1.6 and 3.2 mM. **c** Cell growth under the combined treatment of 0.8 mM diamide plus $Al_2(SO_4)_3$ of 0, 0.05, 0.1, 0.2, 0.4, 0.8, 1.6 or 3.2 mM. The data represent the means of six replicates for each time point with standard deviation too small to be shown

program revealed seven distinct gene clusters (A–G) corresponding to the three specific treatments and the control (Fig. 2). The deletion mutants in Cluster A are sensitive to all three treatments. The deletion *opi3Δ* and to a lesser degree *arv1Δ* and *vps9Δ* did not grow well in the control, suggesting they are essential even in the non-stressed condition. Because both *OPI3* and *ARV1* encode proteins involving in phosphatidylcholine biosynthesis and ergosterol transport, respectively (McGraw and Henry 1989; Tinkelenberg et al. 2000), deletion of the genes would most likely lead to altered plasma membrane in yeast cells, hence resulting in reduced growth and high sensitivity to external stressors like diamide and Al^{3+}. Cluster C also consists of sensitive deletions in the same annotated categories as for Cluster A except all mutants grew well in the control. Among these 24 genes in clusters A and C, 15 were involved in vacuolar and vesicular transport, protein targeting/sorting and translocation (*PEP7*, *PEP3*, *VPS1*, *VPS9*, *VPS33*, *VPS45*, *VPS51*, *VPS52*, *VPS65*, *LUV1*, *SEC66*, *BST1*, *DID4*, *VMA4*, *VMA13*). This indicates that a smooth transportation network by vacuoles and vesicles is a common defense or survival mechanism against detrimental stressors such as diamide and Al^{3+}. Along this reasoning, genes in Clusters B, D and E pointed to a cellular mechanism against Al^{3+} alone. Nineteen deletions were sensitive to Al^{3+} alone and diamide plus Al^{3+}. Their resistance to diamide alone suggests that they are solely related to Al^{3+} sensitivity. Similarly, most of the deletions in

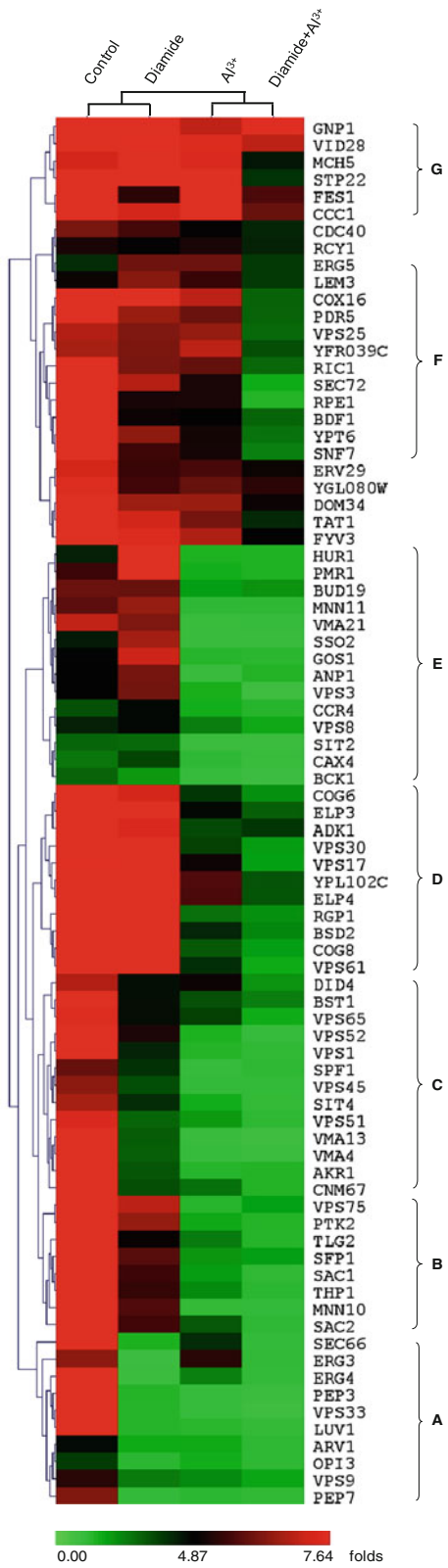

◀**Fig. 2** Cluster analysis of the phenotypic screening data. Cluster analysis of the phenotypic screening data. Four individual treatments (control, 0.8 mM diamide, 0.8 mM $Al_2(SO_4)_3$, 0.8 mM diamide plus 0.4 mM $Al_2(SO_4)_3$) were applied to 81 gene deletion mutants of yeast. The resultant fold change in growth for each mutant in a given treatment was calculated as a ratio of OD_{600} at the end of the treatment over the initial reading. The cluster analysis was carried out using MeV version 4.5 hierarchical clustering program. Seven distinctive clusters (*A*–*G*) were obtained. The fold change data were obtained as the means of two replicates for each mutant

Cluster E are also Al^{3+}-related, except *bck1Δ*, *cax4Δ*, *slt2Δ*, *vps8Δ* and *ccr4Δ*, whose deletion affected normal cell growth as shown by *opi3Δ* and *arv1Δ*.

To delineate the molecular mechanism for diamide-induced Al^{3+} toxicity, the key clues can be derived from the gene deletions which are not affected by either diamide or Al^{3+} alone but by their combination, as demonstrated by Cluster F (*rpe1Δ*, *sec72Δ*, *pdr5Δ* and *ric1Δ*). This is the only cluster of deletion mutants sensitive to the treatment of dual stressors, implying these genes are responsible for the tolerance to diamide-induced Al toxicity because deletion of these genes resulted in sensitivity.

The sensitivity of *RPE1Δ* mutant to diamide-induced Al toxicity indicates the critical role of *RPE1* in the disulfide stress response. This role is most likely related to the generation of nicotinamide adenine dinucleotide phosphate (NADPH), a major cofactor requirement for redox reactions directed against ROS. *RPE1* encodes for a D-ribulose-5-phosphate 3-epimerase in the pentose phosphate pathway (Gorsich et al. 2006), which is the key source of NADPH. *PDR5* is a pleiotropic drug resistance gene, encoding a 160 kDa multidrug transporter Pdr5p which belongs to the ATP-binding cassette (ABC) family (Balzi et al. 1994, Decottignies and Goffeau 1997). Pdr5p has unusual flexibility toward its substrate cargo and can efflux structurally diverse xenobiotic compounds and confer broad-spectrum resistance (Sauna et al. 2008). Pdr5p protein consists of 1,511 amino acids. Among them are 28 cysteine residues. Its bulkiness and multiple cysteine residues make it a ready target for diamide. This point of view is supported by the published data that diamide treatment caused secretion defects and eventual cell wall damage due to improper disulfide bond formation in proteins (Gasch et al. 2000). Metal export is a common detoxification strategy in prokaryotes and a large number of transport proteins catalysing metal

export have been characterized (Silver 1998; Rosen 1999; Nies 2003). The result here clearly suggests that Pdr5p plays a role in Al^{3+} detoxification. Further, we reason that the loss of function for *PDR5* homologue such as *MDR1* in mammalian cells (Balzi et al. 1994) could also trigger Al^{3+} accumulation. *SEC72* and *RIC1* genes are related to protein synthesis and secretion. Their deletion could well disrupt the synthesis and secretion of Rpe1p and Pdr5p, leading to sensitivity to diamide-induced Al^{3+} toxicity. To explore the effect of these gene deletions (*rpe1Δ*, *sec72Δ*, *pdr5Δ* and *ric1Δ*) on vacuole/vesicle and diamide-induced Al^{3+} accumulation, we attempted fluorescent staining for Al^{3+} and confocal microscopy. However, Al^{3+} was found evenly present in the cytoplasma with no discrimination of particular Al^{3+}-accentuated organelles (data not shown).

The yeast mutants in cluster G (Fig. 2) (*gnp1Δ*, *mch5Δ* and *ccc1Δ*, *vid28Δ* and *fes1Δ*) were resistant to Al^{3+} alone, diamide alone, and their combination, suggesting these genes are potential Al^{3+} transporters since their deletion mitigated diamide-induced Al^{3+} toxicity. Interestingly three of them are transporter genes (*GNP1*, *MCH5* and *CCC1*) albeit no literature has identified them as Al^{3+} transporters. The other two (*VID28* and *FES1*) are involved in protein trafficking. The *CCC1* gene was shown to be an iron or manganese transporter in the vacuoles (Li et al. 2001). Its loss might interrupt Al^{3+}uptake rendering the mutant yeast resistance to diamide and Al^{3+}. *GNP1* is a high-affinity glutamine permease, also transporting Leu, Ser, Thr, Cys, Met and Asn (Zhu et al. 1996). Its potential role in Al^{3+} uptake needs to be investigated.

The yeast deletion mutants in cluster F (Fig. 2) (*rpe1Δ*, *sec72Δ*, *pfr5Δ* and *ric1Δ*) were further tested with 0.8 mM diamide plus 0.4 mM Al^{3+} and 0.8 mM diamide plus 0.4 mM Al^{3+} in the presence of 0.4 mM DTT. As shown in Fig. 3a, the growth of these mutants in DTT media had increased 4- to 6-fold compared to the pre-treatment OD_{600} readings. The same experiment was also performed with 3.2 mM ascorbic acid. Ascorbic acid completely reversed the toxicity of 0.8 mM diamide on 0.4 mM Al^{3+} (data not shown). In contrast, *gnp1Δ*, *mch5Δ*, *ccc1Δ* and *fes1Δ* were resistant to diamide plus Al^{3+} and DTT had little effect on their growth (Fig. 3b). This further confirmed the deletion mutant screening data as shown in Fig. 2.

Further ICP-OES analysis using *RPE1* mutant demonstrated that the reversal of diamide-induced

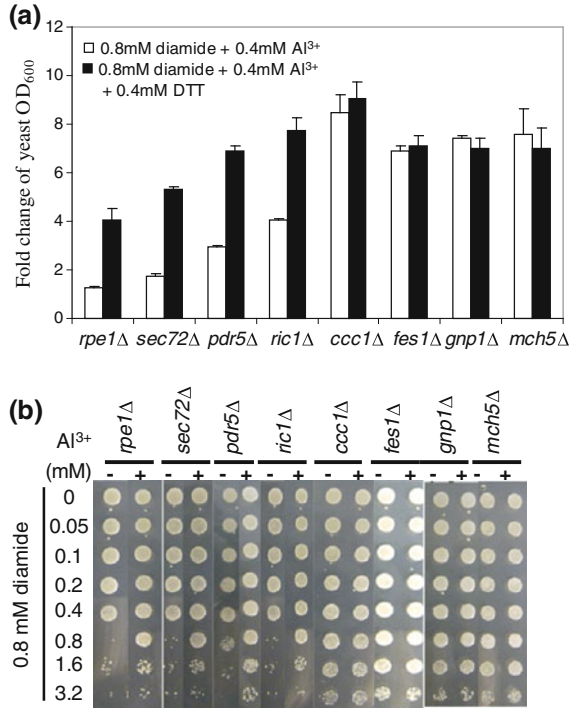

Fig. 3 The effect of DTT on diamide-induced Al^{3+} toxicity. The effect of DTT on diamide-induced Al^{3+} toxicity. **a** The reversal of diamide-induced Al^{3+} toxicity by DTT in liquid culture. The yeast mutants of Clusters F and G were treated with diamide plus Al^{3+}, with and without 0.4 mM DTT, in 96-well microtitre plates. The data represent the means of two replicates for each mutant with standard deviation shown. **b** The reversal of diamide-induced Al^{3+} toxicity by DTT in YPD agar plates. The same mutants as in **a** were analyzed in the same way as in **a** but using agar plate to visualize yeast growth. '−' denotes without 0.4 mM DTT and '+' with 0.4 mM DTT

Al^{3+} toxicity by DTT was associated with the reduction of intracellular Al^{3+} (Fig. 4). *RPE1* mutant at OD_{600} of 0.288 was treated with 0.1 mM Al, 0.8 mM diamide, 0.8 mM diamide plus 0.1 mM Al^{3+}, and 0.8 mM diamide plus 0.1 mM Al^{3+} as well as 0.4 mM DTT, respectively. As shown in Fig. 4a, yeast cells treated with diamide and Al^{3+} had little growth in the 20 h duration in comparison with diamide alone and Al^{3+} alone controls. Addition of 0.4 mM DTT reversed the toxicity by increasing the growth approximately seven times. ICP-OES analysis demonstrated that DTT reduced the cellular Al^{3+} content approximately about sixfold compared to the diamide plus Al^{3+} treated cells (Fig. 4b). The data reinforce the diamide-mediated Al^{3+} toxicity discovery and that the *RPE1*-associated NADPH-generating pentose phosphate pathway, which is important for adaptation to

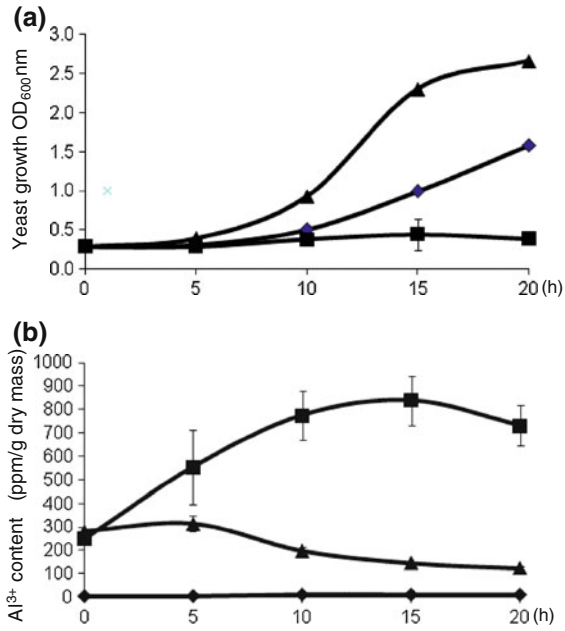

Fig. 4 Al^{3+} accumulation by ICP-OES measurement with *rpe1Δ*. ICP-OES analysis for Al^{3+} content in *rpe1Δ* mutant. **a** Growth curves of *rpe1Δ* cells treated with diamide (*filled diamond*), diamide plus Al^{3+} (*filled square*), diamide plus Al^{3+} and DTT (*filled triangle*). **b** Al^{3+} contents in *rpe1Δ* cells treated with diamide (*filled diamond*), diamide plus Al^{3+} (*filled square*), diamide plus Al^{3+} and DTT (*filled triangle*).The data represent the means of two replicates for each time point with standard deviation shown

hydrogen peroxide (Ng et al. 2008), is also a factor in protection against disulfide stress.

The clear clusters of gene deletion mutants were obtained from the screening data after Al^{3+} or diamide treatment of yeast or treatment with combinations of both. The distinct clustering reflects the unique molecular mechanism the cells use to counter diamide-induced Al^{3+} toxicity. That is, the disruption of Pdr5p, Ric1p and Sec72p mediated detoxification pathway results in Al^{3+} accumulation which in turn leads to the diamide/Al^{3+} sensitive phenotype (Fig. 5). This study has also shown that yeast is adept at balancing redox capacity to avoid the effects of ROS like diamide and the effects of Al such as the involvement of the *RPE1*-related pentose phosphate pathway. Clearly the effects of the stressors can be offset by exogenous addition of reducing agents such as DTT and ascorbate. This immediately brings to mind the stresses that can arise in industrial fermentations—such as in breweries and distilleries, and the application of the findings in this study to the industry.

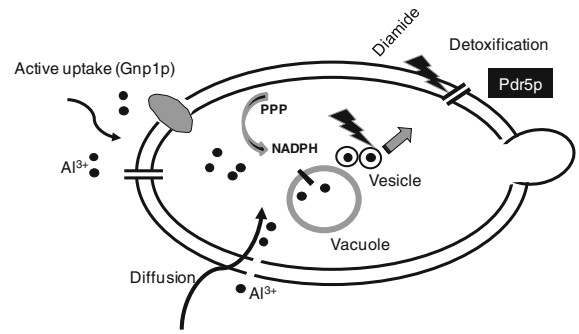

Fig. 5 Proposed molecular mechanism for diamide-induced Al^{3+} toxicity. The proposed molecular mechanism for diamide-induced Al^{3+} toxicity. Al^{3+} uptake can be facilitated by active transport via transporters such as Gnp1p or passive diffusion. Its detoxification is mediated by vesicle/vacuole and plasma membrane-bound Pdr5p. Upon exposure to the thiol-oxidizing agent-diamide, cells firstly mobilize its antioxidant defence system such as pentose phosphate pathway (PPP) which produces NADPH to reduce the oxidant. Any non-reduced diamide would target vesicle/vacuole and Pdr5p detoxification process, leading to Al^{3+} accumulation and toxicity. '⚡' denotes diamide attack

At the other end of the spectrum of usefulness, this study is relevant to medical field. The recent breakthrough on AD using the yeast model (Treusch et al. 2011) reinforced the relevance of yeast model. We believe that these data have deepened our understanding of disulfide stress in eukaryotic organisms and could particularly benefit investigations into Al^{3+}-associated human health problems such as AD.

Acknowledgments This research was supported under Australian Research Council's Linkage Projects funding scheme (project number LP0775238) and the University of Western Sydney for financial support through internal research grant (MW). The authors gratefully acknowledge the support by Foster's Group Limited and thank Kellie McNamara for her technical support.

References

Balzi E, Wang M, Leterme S, Van Dyck L, Goffeau A (1994) *PDR5*, a novel yeast multidrug resistance conferring transporter controlled by the transcription regulator *PDR1*. J Biol Chem 269:2206–2214

Becker PS, Cohen CM, Lux SE (1986) The effect of mild diamide oxidation on the structure and function of human erythrocyte spectrin. J Biol Chem 261:4620–4628

Brachmann CB, Davies A, Cost GJ, Caputo E, Li JC, Hieter P, Boeke JD (1998) Designer deletion strains derived from *Saccharomyces cerevisiae* S288C: a useful set of strains

and plasmids for PCR-mediated gene disruption and other applications. Yeast 14:115–132

Decottignies A, Goffeau A (1997) Complete inventory of the yeast ABC proteins. Nat Genet 15:137–145

Exley C (2006) Aluminium and iron, but neither copper nor zinc, are key to the precipitation of β-sheets of Aβ42 in senile plaque cores in Alzheimer's disease. J Alzheimer's Dis 10:173–177

Gasch AP, Spellman PT, Kao CM et al (2000) Genomic expression programs in the response of yeast cells to environmental changes. Mol Biol Cell 11:4241–4257

Gorsich S, Dien B, Nichols N, Slininger P, Liu Z, Skory C (2006) Tolerance to furfural-induced stress is associated with pentose phosphate pathway genes *ZWF1*, *GND1*, *RPE1*, and *TKL1* in *Saccharomyces cerevisiae*. Appl Microbiol Biotechnol 71:339–349

Kakimoto M, Kobayashi A, Fukuda R, Ono Y, Ohta A, Yoshimura E (2005) Genome-wide screening of aluminum tolerance in *Saccharomyces cerevisiae*. Biometals 18:467–474

Kosower NS, Kosower EM (1995) Diamide: an oxidant probe for thiols. Method Enzymol 251:123–133

Leichert LIO, Scharf C, Hecker M (2003) Global characterization of disulfide stress in *Bacillus subtilis*. J Bacteriol 185:1967–1975

Li L, Chen OS, McVey Ward D, Kaplan J (2001) *CCC1* is a transporter that mediates vacuolar iron storage in yeast. J Biol Chem 276:29515–29519

McGraw P, Henry SA (1989) Mutations in the *Saccharomyces cerevisiae* opi3 gene: effects on phospholipid methylation, growth and cross-pathway regulation of inositol synthesis. Genetics 122:317–330

Nagahara N (2011) Intermolecular disulfide bond to modulate protein function as a redox-sensing switch. Amino Acids 41:59–72

Ng CH, Tan SX, Perrone GG, Thorpe GW, Higgins VJ, Dawes IW (2008) Adaptation to hydrogen peroxide in *Saccharomyces cerevisiae*: The role of NADPH-generating systems and the SKN7 transcription factor. Free Radic Biol Med 44:1131–1145

Nies D (2003) Efflux-mediated heavy metal resistance in prokaryotes. FEMS Microbiol Rev 27:313–339

Rosen B (1999) The role of efflux in bacterial resistance to soft metals and metalloids. Essays Biochem 34:1–15

Saeed AI, Bhagabati NK, Braisted JC et al (2006) TM4 microarray software suite. Method Enzymol 411:134–193

Sauna ZE, Bohn SS, Rutledge R et al (2008) Mutations define cross-talk between the N-terminal nucleotide-binding domain and transmembrane helix-2 of the yeast multidrug transporter *PDR5*: possible conservation of a signaling interface for coupling ATP hydrolysis to drug transport. J Biol Chem 283:35010–35022

Silver S (1998) Genes for all metals - a bacterial view of the periodic table. The 1996 Thom Award Lecture. J Ind Microbiol Biotechnol 20:1–12

Thorpe GW, Fong CS, Alic N, Higgins VJ, Dawes IW (2004) Cells have distinct mechanisms to maintain protection against different reactive oxygen species: Oxidative-stress-response genes. Proc Natl Acad Sci USA 101:6564–6569

Tinkelenberg AH, Liu Y, Alcantara F, Khan S, Guo Z, Bard M, Sturley SL (2000) Mutations in yeast *ARV1* alter intracellular sterol distribution and are complemented by human *ARV1*. J Biol Chem 275:40667–40670

Treusch S, Hamamichi S, Goodman JL et al (2011) Functional links between Aβ toxicity, endocytic trafficking, and Alzheimer's disease risk factors in yeast. Science 334:1241–1245

Walton JR (2006) Aluminum in hippocampal neurons from humans with Alzheimer's disease. NeuroToxicology 27: 385–394

Widestrand J, Lundh T, Pettersson H, Lindberg JE (2003) A rapid and sensitive cytotoxicity screening assay for trichothecenes in cereal samples. Food Chem Toxicol 41: 1307–1313

Wu MJ, O'Doherty PJ, Murphy PA et al (2011) Different reactive oxygen species lead to distinct changes of cellular metal ions in the eukaryotic model organism *Saccharomyces cerevisiae*. Int J Mol Sci 12:8119–8132

Yumoto S, Nagai H, Matsuzaki H, Matsumura H, Tada W, Nagatsuma E, Kobayashi K (2001) Aluminium incorporation into the brain of rat fetuses and sucklings. Brain Res Bull 55:229–234

Zhu X, Garrett J, Schreve J, Michaeli T (1996) *GNP1*, the high-affinity glutamine permease of *S. cerevisiae*. Curr Genet 30:107–114